

A method for gait events detection based on low spatial resolution pressure insoles data

Original

A method for gait events detection based on low spatial resolution pressure insoles data / Salis, F.; Bertuletti, S.; Bonci, T.; Della Croce, U.; Mazza, C.; Cereatti, A.. - In: JOURNAL OF BIOMECHANICS. - ISSN 0021-9290. - ELETTRONICO. - 127:(2021), p. 110687. [10.1016/j.jbiomech.2021.110687]

Availability:

This version is available at: 11583/2927565 since: 2021-10-05T12:27:05Z

Publisher:

Elsevier Ltd

Published

DOI:10.1016/j.jbiomech.2021.110687

Terms of use:

This article is made available under terms and conditions as specified in the corresponding bibliographic description in the repository

Publisher copyright

Elsevier postprint/Author's Accepted Manuscript

© 2021. This manuscript version is made available under the CC-BY-NC-ND 4.0 license
<http://creativecommons.org/licenses/by-nc-nd/4.0/>. The final authenticated version is available online at:
<http://dx.doi.org/10.1016/j.jbiomech.2021.110687>

(Article begins on next page)

A Method for Gait Events Detection based on Low Spatial Resolution Pressure Insoles data

F. Salis^{1,2}, S. Bertuletti^{1,2}, T. Bonci³, U. Della Croce^{1,2}, C. Mazzà³, A. Cereatti^{2,4}

¹Department of Biomedical Sciences, University of Sassari, Sassari, Italy; ²Interuniversity Centre of Bioengineering of the Human Neuromusculoskeletal System, Sassari, Italy; ³Insigneo Institute and Department of Mechanical Engineering, University of Sheffield, Sheffield, UK; ⁴Department of Electronics and Telecommunications, Politecnico di Torino, Torino, Italy.

Authors list:

- 1) Francesca Salis, Department of Biomedical Sciences, University of Sassari, Sassari, Italy; Interuniversity Centre of Bioengineering of the Human Neuromusculoskeletal System, Sassari, Italy; email: fsalis1@uniss.it
- 2) Stefano Bertuletti, Department of Biomedical Sciences, University of Sassari, Sassari, Italy; Interuniversity Centre of Bioengineering of the Human Neuromusculoskeletal System, Sassari, Italy; email: sbertuletti@uniss.it
- 3) Tecla Bonci, Insigneo Institute for in silico Medicine and Department of Mechanical Engineering, University of Sheffield, Sheffield, UK; email: t.bonci@sheffield.ac.uk
- 4) Ugo Della Croce, Department of Biomedical Sciences, University of Sassari, Sassari, Italy; Interuniversity Centre of Bioengineering of the Human Neuromusculoskeletal System, Sassari, Italy; email: dellacro@uniss.it
- 5) Claudia Mazzà, Insigneo Institute for in silico Medicine and Department of Mechanical Engineering, University of Sheffield, Sheffield, UK; email: c.mazza@sheffield.ac.uk
- 6) Andrea Cereatti, Department of Electronics and Telecommunications, Politecnico di Torino, Torino, Italy; email: andrea.cereatti@polito.it

Telephone number (Francesca Salis): +39 3335339646

Fax: +39 079 228520

Keywords:

gait analysis, wearable sensors, pressure insoles, locomotion, gait events

Submitting for:

Short communication

Word Count:

Abstract: 213

Manuscript: 2230

ABSTRACT

The accurate identification of initial and final foot contacts is a crucial prerequisite for obtaining a reliable estimation of spatio-temporal parameters of gait. Well-accepted gold standard techniques in this field are force platforms and instrumented walkways, which provide a direct measure of the foot-ground reaction forces. Nonetheless, these tools are expensive, non-portable and restrict the analysis to laboratory settings. Instrumented insoles with a reduced number of pressure sensing elements might overcome these limitations, but a suitable method for gait events identification has not been adopted yet. The aim of this paper was to present and validate a method aiming at filling such void, as applied to a system including two insoles with 16 pressure sensing elements (element area = 310 mm²), sampling at 100Hz. Gait events were identified exploiting the sensor redundancy and a cluster-based strategy. The method was tested in the laboratory against force platforms on nine healthy subjects for a total of 801 initial and final contacts. Initial and final contacts were detected with low average errors of (about 20 ms and 10 ms, respectively). Similarly, the errors in estimating stance duration and step duration averaged 20 ms and less than 10 ms, respectively. By selecting appropriate thresholds, the method may be easily applied to other pressure insoles featuring similar requirements.

I. INTRODUCTION

The gait cycle represents the functional element of walking, traditionally identified by the initial contact (IC) of the foot with the ground and the following IC of the same foot (Della Croce et al., 2018; Whittle, 1993). A direct approach to detect these gait events (GEs) is by using force platforms (FPs) and instrumented walkways. These provide a direct measure of forces resulting from the foot-ground interaction, thus representing a gold standard for GEs detection. However, both devices are non-portable, expensive and require an appropriate laboratory environment, therefore constraining the analysis to few strides and/or straight walks (Adkin et al., 2000). Moreover, laboratory analysis only allows for the assessment of walking capacity, which should ideally be complemented with continuous daily living measures of mobility performance to obtain a thorough assessment (World Health Organization, 2007; Rochester et al., 2020). In this perspective, wearable inertial measurement units (IMUs) are the key to enable gait analysis in real-world scenarios as GEs can be identified from the accelerations and angular velocities signals recorded by two units attached to the ankles/feet (Mariani et al., 2012; Trojaniello et al., 2014). However, being the latter an indirect method, processing algorithms performance may be affected by errors, and it should, therefore, be regarded as a silver standard solution.

Foot switches are an effective alternative to estimate GEs and their use has been explored in several studies over the last decades (Agostini et al., 2013; Bae et al., 2011; Hausdorff et al., 1995; Kong et al., 2009; Skelly et al., 2001). The foot switch technology, however, generally includes only two or three sensing elements, which require a proper positioning under the foot. Due its low spatial sensor resolution, the approach does not allow to identify the specific area of the sole-ground contact and, in turn, it may also affect the GEs temporal resolution. This is even more true in case of pathological gait (i.e., pronation, supination, equine gait, foot drop, shuffling children with cerebral palsy), for which few sensors are not sufficient (Smith et al., 2016). Another attractive option is represented by plantar pressure insoles, based on different technologies and sensors configurations (e.g., Tekscan® F-Scan® System; Novel® Pedar® System, etc.). However, these devices are specifically conceived for high-resolution pressure mapping applications and generally include a dense grid of sensors (from 99 to 960 sensing elements) which inevitably lead to higher costs and complexity in terms of data management and reading, but which are not strictly necessary for simple GEs estimations.

In this study we propose an original method for GEs detection, based on the use of instrumented insoles, each including only sixteen force-sensing resistor elements (pressure insoles, PIs). The implemented algorithm exploits the number of sensors by using a cluster-based approach to describe foot-ground contacts in a finer way and avoid missed and extra GEs, providing information about foot positioning. The method was tested against FPs in the laboratory using data collected on healthy subjects.

II. METHODS

A. System Description and GEs algorithm

Two plantar PIs (mod. YETI, 221e S.r.l., Padua, Italy; 16 sensing elements; element area = 310 mm²; fs = 100 Hz; ground reaction force threshold = 5 N) were used in this study, with a design similar to that adopted by Ciniglio et al. 2021. Each sensing element is constituted by a force sensing resistor, exhibiting a resistance value inversely

96 proportional to the applied force. The output is expressed as voltage (full-scale voltage value $V_{FS} = 2.8$ V). Each
97 pressure insole is connected to a central processing unit, which also includes a magneto-IMU (Figure 1) that is not
98 used for this study. Data is recorded by an ultra-low-power microcontroller and stored in an on-board flash
99 storage.

100
101 FIGURE 1 ABOUT HERE
102

103 The PI signals processing algorithm is described by the following steps (Figure 2):

104 (i) *Pre-processing.*

105 PI signals are normalised with respect to V_{FS} , expressed in normalised units (nu), and then filtered using a 5-points
106 non-linear median filter to have a smoothing effect while enhancing edges (Stork et al., 2003);

107 (ii) *Detection and selection of instants of rising and falling edges.*

108 For each of the filtered PI signals $X_i(t)$, where $i=1,\dots,16$ represents the i -th PI signal, a first derivative approach
109 (Hopkins, 2001) is applied to detect rising and falling edges. Edges are identified from $\dot{X}_i(t)$ using a peak detection
110 approach (Benocci et al., 2009) with an amplitude threshold defined as $Th_1 = 5n$, being n the signal noise
111 amplitude as computed in static conditions (in this study, we used $Th_1 = 0.05$ nu). For each PI signal, rising edges
112 are identified as positive peaks $> Th_1$ and the corresponding time instants are organized in a vector $t_{RE,j}$. Similarly,
113 falling edges are identified as negative peaks $< -Th_1$ and the corresponding time instants are organized in a vector
114 $t_{FE,j}$. Rising and falling edges are automatically checked, in terms of time distance and amplitude of the PI signal,
115 to discard false positives. Figure 2a shows an example of detection of a rising edge and a falling edge;

116 (iii) *Detection and selection of local minima (instants of rising and falling minima).*

117 The identification of the instants of rising and falling minima is performed by applying to $X_i(t)$ a threshold $Th_2 =$
118 0.02 nu, using rising and falling edges as reference points (Hausdorff et al., 1995). In particular, each rising minima
119 is identified as the first point with $X_i(t) < Th_2$ preceding the considered rising edge instant, while each falling
120 minima is identified as the first point with $X_i(t) < Th_2$ after the considered falling edge instant. Rising minima
121 instants and falling minima instants were organised in vectors, $t_{RM,i}$ and $t_{FM,i}$ respectively. Figure 2a shows an
122 example of detection of one rising minimum and one falling minimum;

123 (iv) *Identification of activation/deactivation clusters.*

124 Once the rising and falling minima instants are detected for all the PI signals, they are organised in chronological
125 order in a unique vector (t_{RM} and t_{FM} respectively), also noting the corresponding sensing element number in
126 another vector (s_{RM} and s_{FM}). This step is needed to group the instants of rising/falling minima corresponding to
127 the same foot contact, i.e. the PI sensing elements which activate/deactivate together when the foot hits the
128 ground. An activation cluster is identified imposing that the time distance between consecutive instants of t_{RM} is
129 lower than $Th_3 = 0.4s$. Then, a deactivation cluster includes the instants of t_{FM} between two consecutive activation
130 clusters. For each cluster, the minima instants and the sensing elements numbers are saved ($A_cluster_j$
131 $/D_cluster_j$, where $j = j$ -th activation/deactivation cluster).

132 Figure 2b shows an example of one activation cluster and one deactivation cluster.

133 (v) *Identification of IC/FC (final contact) intervals and definition of IC/FC events.*

134 A foot-ground contact interval is defined when at least three sensing elements of the PI belonging to the same
135 spatial neighbourhood are consecutively activated and deactivated, i.e. correspond to three consecutive minima
136 belonging to the same cluster ($A_cluster$ for ICs and $D_cluster$ for FCs). For each PI's sensing element, the
137 neighbourhood consists of those sensing elements which are spatially close to the considered unit (Figure 1) (e.g.
138 for the sensing element no. 12, the neighbourhood includes sensing elements 11, 13, 14, 15, 16; further details
139 are reported in *Appendix B*). In fact, it is reasonable to assume that, when an IC or FC occurs, the sensing elements
140 which refer to the same anatomically functional area of foot sole are activated or deactivated, respectively.

141 Each IC interval is identified starting from the first rising minima of an activation cluster; while each FC interval is
142 identified starting from the last falling minima of a deactivation cluster.

143 Finally, each IC is assumed to coincide with the rising minimum instant corresponding to the third sequentially
144 activated sensing elements within the considered IC interval. Likewise, each FC is assumed to coincide with the
145 falling minimum instant corresponding to the third sequentially deactivated sensing elements within the
146 considered FC interval. Figure 2c shows an example of one IC interval and one FC interval.

147 A workflow of the algorithm can be found in *Appendix A*.

148
149 FIGURE 2 ABOUT HERE
150

151 **B. Experimental setup**

152 The validation experiments involved nine healthy participants (5 females and 4 males; age 25.4 ± 1.3 years, shoe
153 size 40.5 ± 4.1 EU) and took place at the University of Sassari (Italy). All participants signed an informed consent
154 approved by the IRB before taking part to the study. PIs were inserted in participants' shoes and central
155 processing units were clipped over the instep (Figure 3). The only specific requirement for the shoes was to avoid
156 knee-high boots. Data from two FPs (AMTI, Massachusetts, USA; $f_s = 1000$ Hz) were acquired through a motion
157 capture system also including video recordings (Vicon Vue, $f_s = 50$ Hz). Data from PIs and FPs were synchronized
158 using an additional central processing unit as external trigger, connected to the motion capture system via cable.
159 Each participant was asked to walk for six minutes back and forth at comfortable speed, stepping on the FPs as
160 many times as possible.

161
162 FIGURE 3 ABOUT HERE
163

164 **C. Data processing**

165 For each subject, a preliminary visual inspection of the "good strides" (entire foot on the FP during stance phase)
166 was performed using video recordings. Then, FP data were down-sampled to 100 Hz. A pre-processing procedure
167 was applied for the synchronisation of PIs measurements (started via BLE protocol, v. 4.1) with the FP data, using
168 the time vector provided by the trigger to interpolate the data.
169 The GEs detection algorithm results were compared with those obtained from the FPs (ground reaction force
170 threshold = 25 N) in terms of average root mean square (RMS) error, bias and standard deviation (SD) error
171 computed over the stances of all participants. An example of IC and FC detection from both PI and FP is shown in
172 Figure 4.

173
174 FIGURE 4 ABOUT HERE
175

176 **III. RESULTS**

177 RMS error, bias and SD error obtained from the comparison are reported in Table 1. A total of 801 ICs and 801
178 FCs were analysed (89 ICs and FCs on average for each participant), while errors on step duration were computed
179 considering 315 steps in total. Average errors were lower than 10 ms for FCs, 20 ms for ICs, 20 ms for stance
180 duration, less than 1 ms for step duration.

181
182 (Table 1)
183

184 **IV. DISCUSSION**

185 GEs and temporal parameters obtained from the PIs showed a 100% correspondence with those estimated from
186 the FPs. Low average RMS errors were obtained for stance duration (< 20 ms) and for both IC and FC events, (22
187 ms and 17 ms, respectively). IC events, as detected by the proposed method were, on average, anticipated with
188 respect to those detected by the FP (average bias = 21 ms), while FC events were marginally delayed. A bias of 23
189 ms was obtained for stance duration. Very low values were obtained for the average SD error (7 ms for ICs, 12 ms
190 for FCs and 7 ms for stance duration). For step duration, both RMS error and SD error were around one sample,
191 while the average bias was zero.

192 Similar but slightly larger errors were reported by Catalfamo and colleagues (2008) using a F-Scan Mobile Tekscan
193 pressure insole (22 ± 9 ms for ICs and 10 ± 4 ms for FCs). However, it should be noted that the proposed algorithm
194 was successful in obtaining lower errors using a pressure insole with a much smaller number of sensing elements
195 (16 vs 960) and using a lower sample-frequency (100 Hz vs 200 Hz), with clear advantages in terms of cost and
196 efficiency.

197 In general, the majority of the methodological studies analysing the performance of different pressure insoles,
198 focused on gait parameters other than ICs and FCs and reported larger errors (Agarwal et al., 2020; Braun et al.,
199 2015; Carbonaro et al., 2016; Crea et al., 2014). For instance, the average error reported in Carbonaro et al. (2016)
200 by comparing a commercial smart shoe including two force sensors (FootMov) against a motion capture system
201 was 39 ± 65 ms for stance duration. Often, a direct comparison with the results in the literature was not possible

202 due to the lack of a gold standard (Benocci et al., 2009), adoption of manual labelling of the GE detection (Roth
203 et al., 2018) or different research objectives (i.e., PI signals used only for activity recognition).
204 The low errors found for both ICs and FCs demonstrated that the combined use of low-cost PI and specific
205 algorithms for signal processing are a good compromise between more complex solutions, such as high-resolution
206 pressure mapping technology, and foot-switch systems with a low number of sensors. A notable feature of the
207 proposed method is that it can be applied to other PIs having a sufficient number of sensing elements. The
208 minimum sensor number and area would clearly depend on the shoe size of the subjects to analyse (e.g. children),
209 however, we found that an activated/deactivated area of about 900 mm² (area of three sensing unit of the PI)
210 guaranteed for good results for both male and female adults. Having a sufficiently high number of sensors allows
211 to describe the foot-ground contact in a comprehensive way and virtually recognise all the possible strategies of
212 foot-floor contact. Last but not least, the PIs here used can be easily combined with IMUs as part of a multi-sensor
213 wearable system, which could provide accurate temporal estimates and a for a more extensive gait assessment
214 also in a free-living context. Further studies will focus on overcoming the limitations of having tested the proposed
215 method only on healthy subjects and on straight walking.
216

217 **V. ACKNOWLEDGEMENT**

218 The work was supported by the MOBILISE-D (EU H2020, EFPIA, and IMI 2 Joint Undertaking; Grant no. 820820),
219 the UK EPSRC (K03877X/1 and S032940/1) and the NIHR Sheffield BRC. The study sponsors were not involved in
220 the study phases, in the writing of the manuscript and in the decision about its submission.

221 **VI. CONFLICT OF INTEREST STATEMENT**

222 The authors declare that there are no financial nor personal relationships that can lead to conflicts of interest.
223

224 **VII. REFERENCES**

- 225 el Achkar, C. M., Lenoble-Hoskovec, C., Paraschiv-Ionescu, A., Major, K., Büla, C., Aminian, K., 2016. Instrumented
226 shoes for activity classification in the elderly. *Gait & posture*, 44, 12-17.
- 227 Adkin, A. L., Frank, J. S., Carpenter, M. G., Peysar, G. W., 2000. Postural control is scaled to level of postural threat.
228 *Gait & Posture*, 12.2, 87–93.
- 229 Agarwal, R., Aggarwal, A., & Gupta, R., 2020. A Wireless Sensorized Insole Design for Spatio-Temporal Gait
230 Analysis. *Neurophysiology*, 52.3, 212-221.
- 231 Agostini, V., Balestra, G., Knaflitz, M., 2013. Segmentation and classification of gait cycles. In *Proceedings of IEEE*
232 *Transactions on Neural Systems and Rehabilitation Engineering*, 22.5, 946-952.
- 233 Bae, J., Tomizuka, M., 2011. Gait phase analysis based on a Hidden Markov Model. *Mechatronics*, 21.6, 961-970.
- 234 Benocci, M., Rocchi, L., Farella, E., Chiari, L., Benini, L., 2009. A Wireless System for Gait and Posture Analysis
235 Based on Pressure Insoles and Inertial Measurement Units. In *Proceedings of the 3rd International*
236 *Conference on Pervasive Computing Technologies for Healthcare*, 1–6.
- 237 Braun, B. J., Veith, N. T., Hell, R., Döbele, S., Roland, M., Rollmann, M., ... Pohlemann, T., 2015. Validation and
238 reliability testing of a new, fully integrated gait analysis insole. *Journal of foot and ankle research*, 8.1, 1-7.
- 239 Carbonaro, N., Lorussi, F., & Tognetti, A., 2016. Assessment of a smart sensing shoe for gait phase detection in
240 level walking. *Electronics*, 5.4, 78.
- 241 Catalfamo, P., Moser, D., Ghousayni, S., Ewins, D., 2008. Detection of gait events using an F-Scan in-shoe pressure
242 measurement system. *Gait & posture*, 28.3, 420-426.
- 243 Ciniglio, A., Guiotto, A., Spolaor, F., Sawacha, Z., 2021. The design and simulation of a 16-sensors plantar pressure
244 insole layout for different applications: From sports to clinics, a pilot study. *Sensors*, 21.4, 1450.
- 245 Crea, S., Donati, M., De Rossi, S. M. M., Oddo, C. M., Vitiello, N., 2014. A wireless flexible sensorized insole for gait
246 analysis. *Sensors*, 14.1, 1073-1093.
- 247 Della Croce, U., Cereatti, A., Mancini, M., 2018. Gait parameters estimated using inertial measurement units. In:
248 Müller, B., Wolf, S. I., Brüggemann, G. P., Deng, Z., McIntosh, A. S., Miller, F., & Selbie, W. S. (Eds), *Handbook*
249 *of human motion*. Springer International Publishing, 245-265.
- 250 Hausdorff, J. M., Ladin, Z., Wei, J. Y., 1995. Footswitch system for measurement of the temporal parameters of
251 gait. *Journal of biomechanics*, 28.3, 347-351.
- 252 Hopkins, D. W., 2001. What is a Norris derivative?. *NIR news*, 12.3, 3-5.

253 Kong, K., Tomizuka, M., 2009. A gait monitoring system based on air pressure sensors embedded in a shoe. In
254 Proceedings of IEEE/ASME Transactions on mechatronics, 14.3, 358-370.

255 Mariani B, Rochat S, Büla CJ, Aminian K., 2012. Heel and toe clearance estimation for gait analysis using wireless
256 inertial sensors. In Proceedings of the IEEE transactions on bio-medical engineering, 59.11, 3162-8.

257 Novel® Pedar® System Web Page. Url: <http://www.novel.de>

258 Panebianco, G. P., Bisi, M. C., Stagni, R., & Fantozzi, S., 2018. Analysis of the performance of 17 algorithms from
259 a systematic review: Influence of sensor position, analysed variable and computational approach in gait
260 timing estimation from IMU measurements. *Gait & posture*, 66, 76-82.

261 Rochester, L., Mazzà, C., Mueller, A., Caulfield, B., McCarthy, M., Becker, C., ... & Mobilise-D Consortium, 2020. A
262 roadmap to inform development, validation and approval of digital mobility outcomes: the Mobilise-D
263 approach. *Digital Biomarkers*, 4.1, 13-27.

264 Roth, N., Martindale, C. F., Eskofier, B. M., Gaßner, H., Kohl, Z., Klucken, J., 2018. Synchronized sensor insoles for
265 clinical gait analysis in home-monitoring applications. *Current Directions in Biomedical Engineering*, 4.1,
266 433-437.

267 Skelly, M. M., Chizeck, H. J., 2001. Real-time gait event detection for paraplegic FES walking. In Proceedings of
268 IEEE Transactions on neural systems and rehabilitation engineering, 9.1, 59-68.

269 Smith, B. T., Coiro, D. J., Finson, R., Betz, R. R., McCarthy, J., 2002. Evaluation of force-sensing resistors for gait
270 event detection to trigger electrical stimulation to improve walking in the child with cerebral palsy. In
271 Proceedings of IEEE Transactions on Neural Systems and Rehabilitation Engineering, 10.1, 22-29.

272 Stork, M., 2003. Median filters theory and applications. In Proceedings of the third International Conference on
273 Electrical and Electronics Engineering Papers-Chamber of Electrical Engineering, Bursa, Turkey, 1-5.

274 Tekscan® F-Scan® System Web Page. Url: <http://www.tekscan.com>

275 Trojaniello, D., Cereatti, A., Pelosin, E., Avanzino, L., Mirelman, A., Hausdorff, J. M., Della Croce, U., 2014.
276 Estimation of step-by-step spatio-temporal parameters of normal and impaired gait using shank-mounted
277 magneto-inertial sensors: application to elderly, hemiparetic, parkinsonian and choreic gait. *Journal of
278 neuroengineering and rehabilitation*, 11.1, 1-12.

279 Whittle, Michael W., 1993. Gait analysis. In: Butterworth-Heinemann (Eds), *The soft tissues.*, 187-199.

280 World Health Organization, 2007. International Classification of Functioning, Disability, and Health: Children &
281 Youth Version: ICF-CY. World Health Organization.

282

283

284

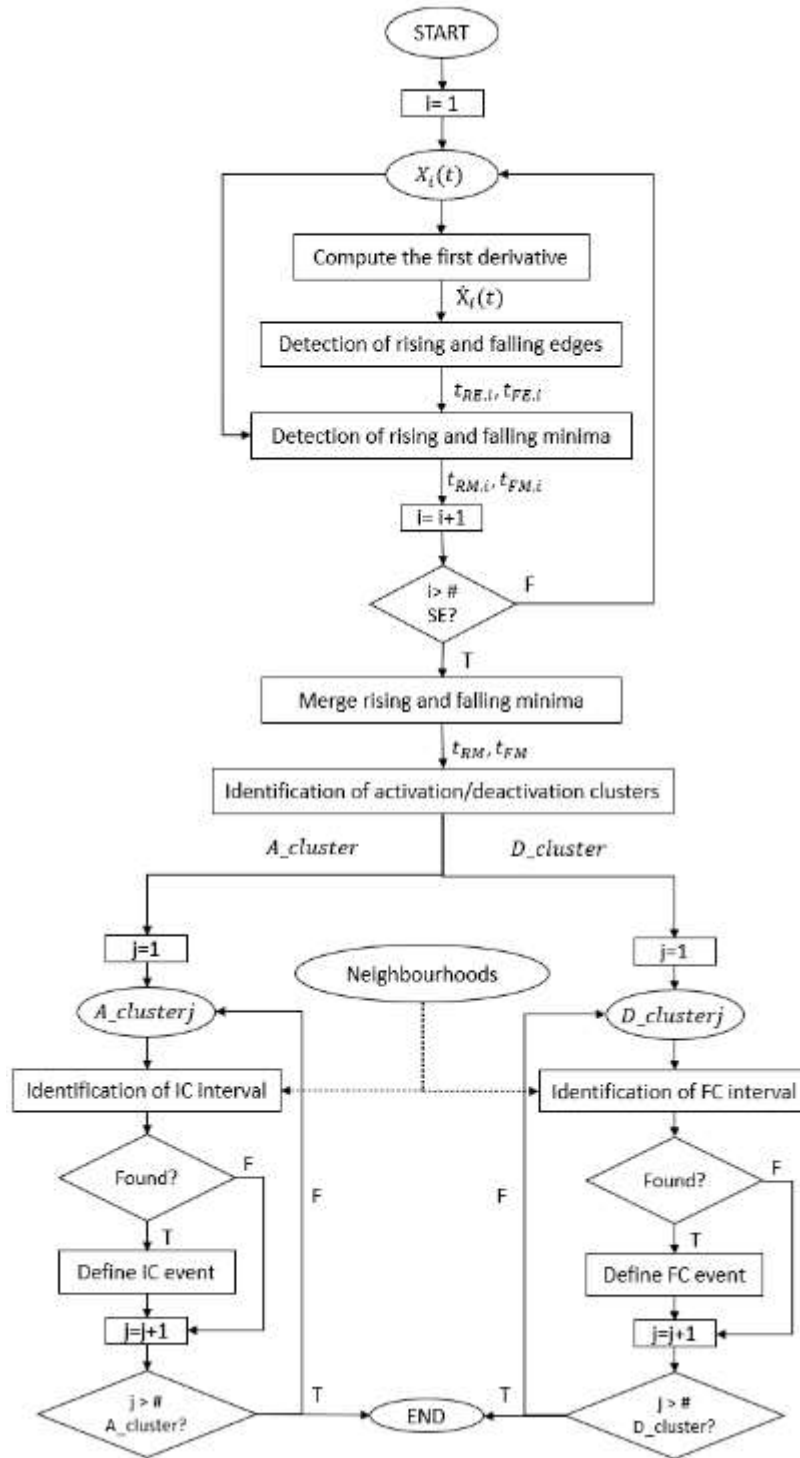


Figure 1. Algorithm workflow

- 286
 287 Definitions:
 288 $X_i(t)$ = pre-processed signal from the i -th sensing element
 289 #SE = number of sensing elements of the pressure insole
 290 $\dot{X}_i(t)$ = first derivative of $Xp_i[n]$
 291 $t_{RE,i}$ = rising edges instants
 292 $t_{FE,i}$ = falling edges instants
 293 $t_{RM,i}$ = rising minima instants
 294 $t_{FM,i}$ = falling minima instants
 295 t_{RE} = rising minima instants of all the sensing units

296 t_{FE} = falling minima instants of all the sensing units

297 A_cluster = activation clusters

298 D_cluster = deactivation clusters

299

300 Checks on rising and falling edges instants:

301 • Check on temporal distance. This is performed applying a threshold $Th_d = 0.6$ s. If the distance between
302 consecutive events is lower than Th_d , the second event is discarded in case of rising edges, while the
303 first event is discarded for the falling edges.

304 • Check on the amplitude reached by $x_i(t)$ after each rising edge instant and before each falling edge
305 instant. The amplitude reached in the considered window (10 samples after a rising edge instant or 10
306 samples before a falling edge instant) must be at least 0.3 nu, otherwise the event is discarded.

307

308

309

310

311

312

313

314

315

316

317

318

319

320

321

322

323

324

325

326

327

328

329

330

331

332

333

334

335

336

337

338

339

340

341

342

343

344

345

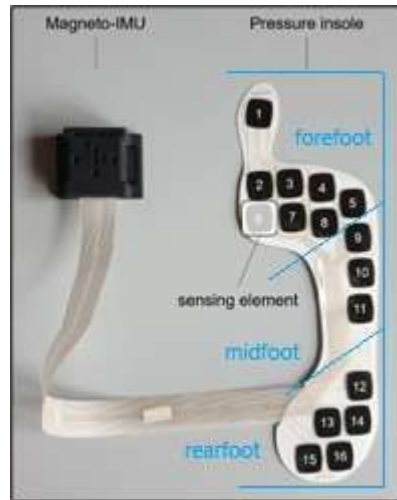
346

347

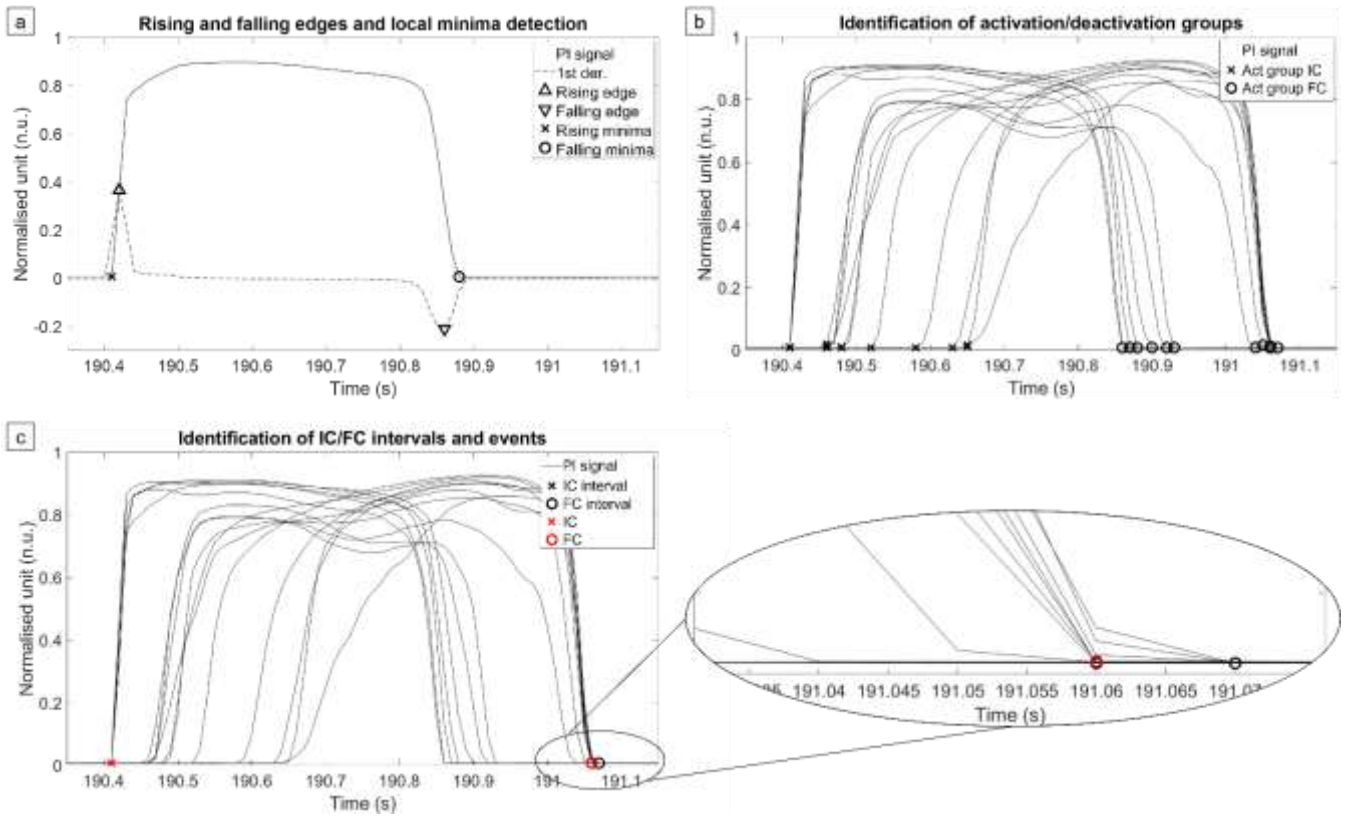
348

349

350



378
 379 Figure 1: Magneto-IMU and pressure insole used for the right foot.
 380
 381

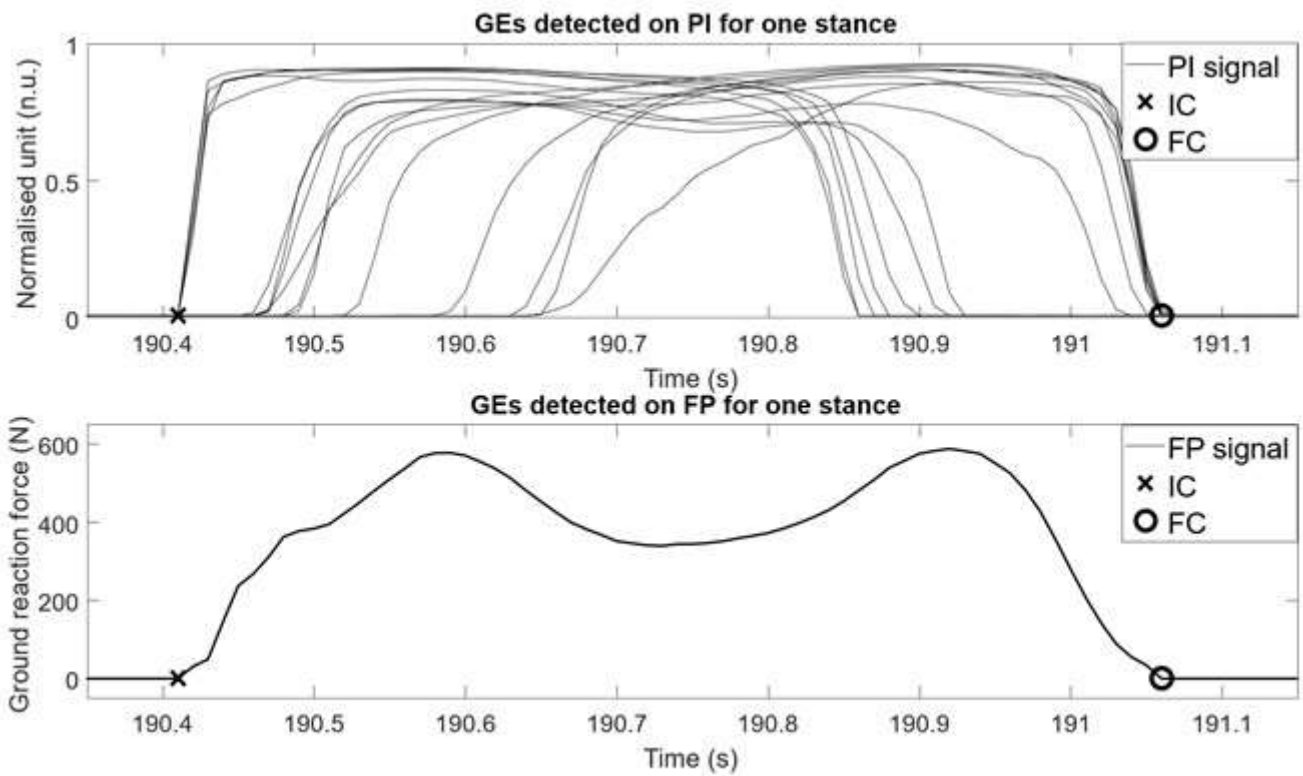


382
 383 Figure 2: Principal steps of the algorithm shown for one stance. a) Detection and selection of rising and falling
 384 edges and local minima (rising and falling minima) for each PI signal; b) Identification of one
 385 activation/deactivation cluster on PI signals; c) Identification of IC/FC intervals and definition of IC and FC events
 386 on PI signals.
 387
 388
 389
 390



391
392
393
394
395

Figure 3: a) PI positioning inside the shoe; b) Clip attached to shoe laces; c) Final sensors positioning with magneto-IMU fixed to the clip.



396
397
398
399
400
401
402
403

Figure 4: Gait events (GEs) detection from both pressure insole (PI) and force plate (FP).

Table 1: RMS error, bias, and SD error

Variable	Average RMS Error (ms; frames)	Average Bias (ms; frames)	Average SD Error (ms; frames)
IC	22; 2	-21; -2	7; <1
FC	18; <2	3; <1	12; 1
Stance duration	18; <2	23; 2	7; <1
Step duration	10; 1	0; <1	10; 1

404